

Electrical conductivity and dielectric characteristics of in situ prepared PVA/HgS nanocomposite films

Omed Gh. Abdullah¹ · Yahya A. K. Salman² · Salwan A. Saleem²

Received: 4 October 2015 / Accepted: 7 December 2015 / Published online: 12 December 2015
© Springer Science+Business Media New York 2015

Abstract Polyvinyl alcohol (PVA) and mercury sulfide (HgS) polymer nanocomposite were prepared using the solution casting and the in situ chemical reduction of mercury nitrate ($\text{Hg}(\text{NO}_3)_2$) and sodium sulfide (Na_2S) in aqueous solutions of PVA as capping for different molar content of $\text{Hg}(\text{NO}_3)_2$ and Na_2S . The nanocomposites films were characterized by Fourier transform infrared, X-ray diffraction (XRD), and scanning electron microscopy. The XRD results for the nanoparticles revealed the hexagonal structure of the HgS, (α -phase). The influence of embedded HgS nanoparticles on the conductivity and dielectric properties of PVA films are investigated, over the frequency range 1 kHz–1 MHz, and the temperature range 30–110 °C. The variation of ac-conductivity with a frequency of the films follows Jonscher's universal power law and found to be increased with increasing temperature, frequency and nanoparticle content. The variation of frequency exponent (s) indicated that the conduction mechanism was correlated barrier hopping model. The dielectric constant (ϵ'), and dielectric loss (ϵ'') was found to decrease with increasing frequency, but increase with increasing temperature and HgS nanoparticles content. The dc-conductivity (σ_{dc}) increase with increase of HgS concentration, and follows Arrhenius behavior in the investigated temperature region.

1 Introduction

It is well known that the addition of inorganic nanoparticles to polymers allows the modification of polymers' physical properties, as well as the implementation of new features in the polymer matrix [1]. When particle sizes decrease to a nanometre scale, the quantum confinement effects and a large surface to volume ratios make these applications even more significant [2]. In particular, HgS nanoparticle has a potential use in solid-state solar cells and photoelectrochemical cells [3]. Thus, synthesis and the effect of this nanoparticle on the polymer are of continuing interest.

The optical and electrical properties of the polymers can be improved to a desired limit through suitable nano fillers, and controlling its concentration [4]. Among the polymers, Polyvinyl alcohol (PVA) is a polymer that has been studied intensively because of its excellent film-forming ability, chemical resistance, and good insulating material [5–7]. PVA has carbon chain backbone with hydroxyl groups attached to methane carbons. These OH groups are sources of hydrogen bonding and hence of assistance information of polymer complexes [8, 9]. PVA has numerous applications in electronics, packaging, textile, and food packaging due to its easy formability, high clarity, excellent durability, and it is thermally stable over a long range of temperature. PVA is a good insulating material with low conductivity and hence, excellent charge storage capacity. Its electrical conductivity depends on the thermally generated carriers [10].

The study of dielectric properties as a function of temperature and frequency is one of the most convenient methods of investigating the structure of polymer nanocomposite [11]. The polarization of a dielectric material is contributed by the electronic, ionic, and dipolar polarization. Electronic and ionic polarization occurs

✉ Omed Gh. Abdullah
omed.abdullah@univsul.edu.iq

¹ Department of Physics, Faculty of Science and Science Education, School of Science, University of Sulaimani, Kurdistan Region, Iraq

² Department of Physics, College of Science, University of Mosul, Mosul, Iraq

during a very short interval of time, while the dipole polarization requires relatively longer time [12]. In case of polar polymers, the dielectric constant values decreased with increasing frequency because when the applied field frequency increased, it was assumed that the permanent dipoles cannot reorient themselves fast enough, and therefore dielectric constant decreases [13]. The understanding of the impact of the inorganic nano fillers on the conduction and electrical properties of the polymer is still a work in progress.

In the present work, Polyvinyl alcohol (PVA) based nanocomposite films, with different concentrations of mercury sulfide (HgS) nanoparticles were prepared by in situ reduction of $\text{Hg}(\text{NO}_3)_2$ and Na_2S in an aqueous PVA solution, using casting technique. The main purpose of this work is to achieve a deeper insight into electrical, and fundamental characterization of PVA films doped with different concentration of synthesized HgS nanoparticle, over a frequency domain from 1 kHz to 1 MHz and within temperature range 30–110 °C.

2 Materials and experiments

2.1 Materials

The raw materials used in the present study were mercury nitrate ($\text{Hg}(\text{NO}_3)_2$) with molecular weight (324.60 g/mol) supplied by Merck, Sodium sulphide nonahydrate ($\text{Na}_2\text{S}\cdot 9\text{H}_2\text{O}$) with molecular weight (240.18 g/mol) supplied by Sigma-Aldrich, polyvinyl alcohol (PVA) (98–99 % hydrolyzed, low molecular weight) supplied by Alfa Aesar, and distilled water as solvent. These materials were used without further purification.

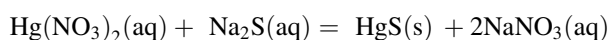
2.2 Preparation of PVA/HgS nanocomposites

In the present system 2 g of PVA was dissolved in 30 mL distilled water using a magnetic stirrer for 1 h at 90 °C until highly homogenous and clean viscous polymer solution was formed. Mercury nitrate ($\text{Hg}(\text{NO}_3)_2$) as Hg^{+2} source and Sodium sulfide (Na_2S) as S^{-2} source, were dissolved in the 5 mL distilled water separately with different molar concentrations (0, 0.01, 0.02, 0.03 and 0.04) M at ambient temperature. Then the two solutions with ration 1:1, were added dropwise to the homogeneous aqueous solution of PVA at 40 °C under stirring, resulting in the change of color of the solution from colorless to dark red, which indicated that the formation of HgS nanoparticle had begun. For maximum dispersion, the mixture was further stirred continuously for (15 min) without heating until homogeneous solutions were obtained. Then the solution was sonicated at 50 % amplitude for 1 s on and 2 s off for total time 3 min.

Table 1 The composition of PVA/HgS nanocomposites films

HgS (M)	PVA (g)	$\text{Hg}(\text{NO}_3)_2$ (g)	Na_2S (g)
0	2	0	0
0.01	2	0.01623	0.012011
0.02	2	0.03246	0.024022
0.03	2	0.04869	0.036034
0.04	2	0.06492	0.048045

These homogeneous solutions were cast in a plastic Petri dish (diameter of 5 cm). The whole assembly was placed in a dust free chamber, and the solvent was allowed to evaporate in the open air at room temperature for a week for nanocomposite films to form. The dried films were peeled off and transferred into desiccators for continuous drying. The chemical reaction for the HgS formation is given by:



The prepared films were free from air bubbles and uniform thickness of the range from 0.06 to 0.10 mm. Table 1 shows the composition of the prepared samples.

2.3 Characterization techniques

The Fourier transform infrared (FTIR) spectra of the pure PVA and nanocomposites samples were analyzed in the range 400–4000 cm^{-1} using a Perkin Elmer in the transmission mode at a resolution of 1.0 cm^{-1} .

The X-ray diffraction (XRD) patterns of the pure PVA film and the PVA/HgS polymer nanocomposite films were recorded using X-ray diffractometer (XPRT-PRO) equipped with Cu $\text{K}\alpha$ as a radiation source ($\lambda = 0.154$ nm) in the 2θ range (10°–70°) at a scanning rate of 2°/min, to report the information about their structure.

The SEM micrograph was taken using (CamScan 3200) to investigate the morphological appearance of the samples.

The electrical measurements were performed using precision LCR Meter (Agilent/HP 4284A) covering a frequency range from 1 kHz to 1 MHz, in the temperature range 30–110 °C. The 2.5 cm diameter films were sandwiched between two stainless steel electrodes under spring pressure. The temperature was measured with a K-type thermocouple having an accuracy of ± 0.1 °C.

3 Results and discussion

3.1 FTIR spectroscopic analysis

Fourier transform infrared spectroscopy (FTIR) is one of the most powerful techniques to investigate a multi-component system, such as polymer nanocomposites because it provides information for both compositions. The FTIR

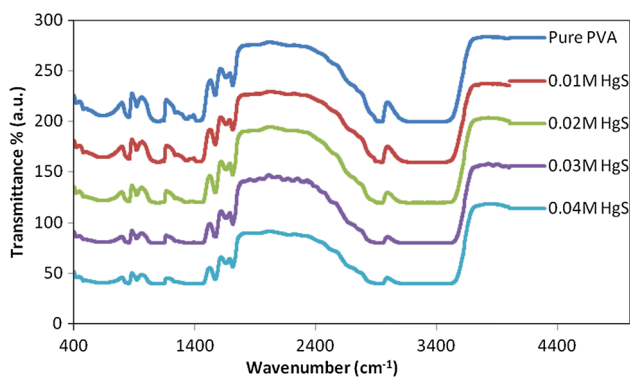


Fig. 1 FTIR spectra of pure PVA, and PVA/HgS nanocomposite films

spectra for pure PVA, and PVA/HgS nanocomposite films are shown in Fig. 1. In case of pure PVA, a strong broad band centered at 3340 cm^{-1} is assigned to the O–H stretching vibration of hydroxyl groups [14]. The strong band at 2942 cm^{-1} is assigned to the band of asymmetric CH_2 stretching vibration [15]. The two bands observed at 1713 , and 1659 cm^{-1} are assigned to C=O and C=C stretching vibrations, respectively [16, 17]. The two bands found at 1427 , and 1331 cm^{-1} are assigned to CH_3 bending vibration and CH_2 stretching respectively [18]. The band at 1092 cm^{-1} arises from the C–O stretching vibration while the band at

918 cm^{-1} results from CH_2 rocking vibration [19]. The band at 852 cm^{-1} results from C–C stretching vibration and that at 652 cm^{-1} arises from CH out of plane bending vibrations [20]. The FTIR spectrum of PVA/HgS nanocomposite samples, shows the observed peak of -OH group of PVA is shifted to lower wavenumber, which indicate the interaction between -OH group and HgS nanoparticles [21]. Also, the spectra showed a decrease in the intensity of all the bands in nanocomposite samples indicating the charge-transfer complex between PVA molecules and HgS nanoparticles [22].

3.2 Scanning electron microscopy (SEM) analysis

Figure 2 shows an example of the scanning electron microscopy (SEM) images of PVA/HgS polymer nanocomposite samples with different HgS concentrations, where white spots indicate HgS that shows almost homogeneous dispersion. It is clear that the increase in mercury nitrate and sodium sulfide concentrations causes the development of HgS average particle sizes due to the agglomeration of the nanoparticles [9, 23].

3.3 X-ray diffraction (XRD) analysis

The formation of PVA/HgS nanocomposite was also confirmed using XRD analysis. Figure 3 depicts the XRD

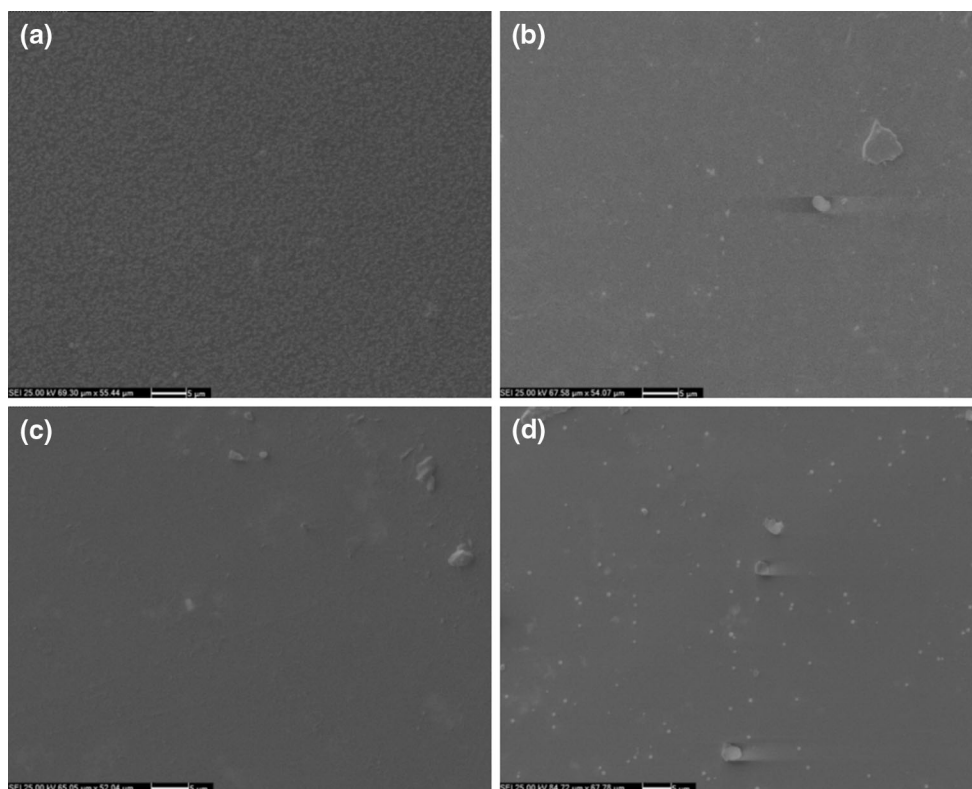


Fig. 2 SEM images of PVA/HgS films **a** 0.01 M HgS, **b** 0.02 M HgS, **c** 0.03 M HgS and **d** 0.04 M HgS

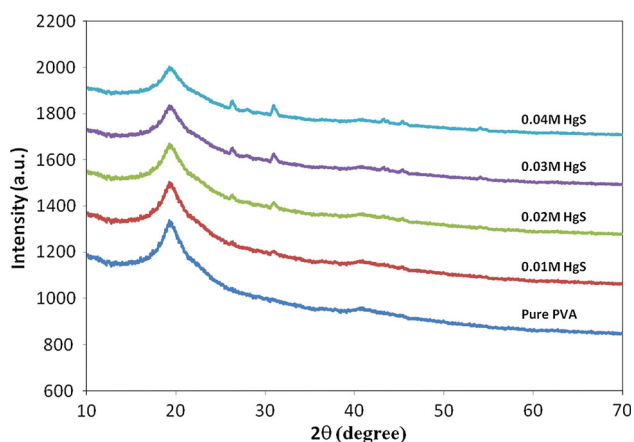


Fig. 3 The X-ray diffractogram of pure PVA, and PVA/HgS nanocomposite

pattern of pure PVA film with different molar concentrations (0, 0.01, 0.02, 0.03 and 0.04) M of HgS films. The first peak observed at $2\theta \approx 19.26^\circ$ for all samples is due to the PVA matrix [24]. On account of HgS nanoparticles embedding the H-bond and –OH group of PVA chains may break and molecular chains are free to rotate [22]. The observed additional small diffraction peaks at scattering angle $2\theta = 26.35^\circ, 27.33^\circ, 30.95^\circ, 43.27^\circ, 45.37^\circ,$ and 54.07° of the nanocomposite samples, are corresponding to reflections from (101), (003), (012), (110), (104) and (202) crystal planes, confirmed the formation of the HgS nanoparticles in a PVA matrix. The X-ray diffraction patterns were indexed and compared with (JCPDS card no. 06-0256) that correspond to the hexagonal phase of HgS (cinnabar) [25, 26]. The diffraction peaks that attributed to HgS is very small compared with that of PVA because the concentration of HgS is very low compared with that of PVA. The intensity of these smaller peaks increases with increasing the HgS concentration.

The crystallite sizes of HgS in nanocomposite films have been determined using Debye–Scherrer formula [27].

$$D = \frac{0.9\lambda}{\beta \cos \theta} \quad (1)$$

where ($\lambda = 0.154$ nm) is the wavelength of X-ray for Cu $K\alpha$ as radiation source, β is the full width at half maximum intensity of the diffraction peak (FWHM), θ is the Bragg diffraction angle of the XRD peak, and D is the particle diameter.

Based on Debye–Scherrer equation, for main peak with $2\theta = 30.95^\circ$ the average crystalline sizes of HgS nanoparticles in PVA/HgS nanocomposite films were estimated. The particle diameter slightly increased from 13.28 to 16.23 nm by increasing the concentration of HgS from 0.01 to 0.04 M.

3.4 Dielectric properties

The dielectric constant and dissipation factor are crucial parameters required in the design of electronic devices. The broadband dielectric spectroscopy has proven to be a very useful tool to study the structure, dynamics and relaxations of polymeric systems. The complex dielectric constant is a material property depending on frequency, temperature, conductivity, size, shape, and spatial arrangement of the constituents (the filler and the matrix), [11, 28]. The dielectric parameters as a function of angular frequency ($\omega = 2\pi f$) is described by the complex dielectric constant in the form;

$$\varepsilon^*(\omega) = \varepsilon'(\omega) - i\varepsilon''(\omega) \quad (2)$$

where, the real part $\varepsilon'(\omega)$ is the dielectric constant which is related to the energy stored in the material, and imaginary part $\varepsilon''(\omega)$. is dielectric loss which is proportional to the energy dissipate in each cycle of the electric field [29].

The measured capacitance, $C(\omega)$. was used to calculate the dielectric constant, $\varepsilon'(\omega)$. using the following expression:

$$\varepsilon'(\omega) = C(\omega)d/\varepsilon_0A \quad (3)$$

where, d is the thickness of the film sample, A is the surface aa of the electrode, and ε_0 is the free space permittivity (8.854×10^{-12} F/m).

The imaginary part of dielectric constant (ε'') is called the loss factor and is a measure of how dissipative or lossy a material to an external electric field. The value of (ε'') is always greater than zero and is usually much smaller than (ε').

The dielectric properties have been analyzed in terms of frequency, temperature, and compositions. Figure 4a, b shows the variation of dielectric constant (ε'), and dielectric loss (ε'') as a function of frequency for different HgS concentrations at 30 °C. It is observed from the figures that t dielectric constants continuously decrease with increasing frequency, which confirms the dielectric dispersion in these materials. The variations of dielectric peters with frequency can be explained in terms of the relaxation time; at low frequencies, the electric dipoles in macromolecules have sufficient time to align with the field before the field changes its direction; consequently, the dielectric constant is high. However, in the high frequency range the dipoles will hardly be able to orient themselves in the direction of the applied field, and hence the value of the dielectric constant decreases [30, 31].

It can be seen from Fig. 4, that (ε') and (ε'') increases with increasing HgS concentration. This can be understood in terms of changes in crystallinity and the degree of cross-linking (the same conclusion was drawn from the diffraction pattern of XRD). Crystallization prevents the movement of the molecular chains; the crystalline phase is rigid and shows no dielectric relaxation processes and, consequently,

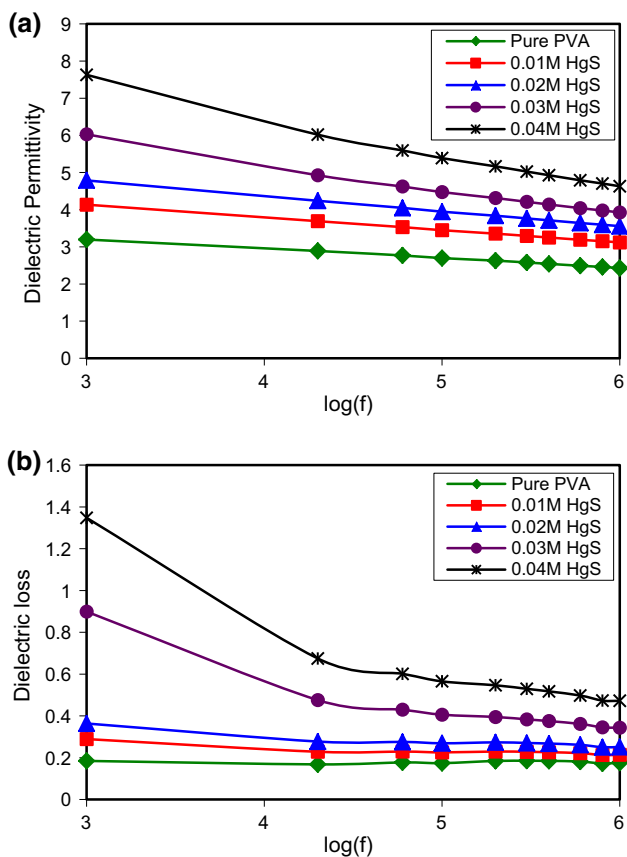


Fig. 4 Variation of **a** dielectric constant (ϵ'), and **b** dielectric loss (ϵ'') as a function of frequency for different HgS concentrations at 30 °C

the dielectric response is lower [32]. The less cross-linking in the sample caused the increase in the number of dipoles, and hence the increase of the dielectric parameters. The dielectric constant of the material directly depends upon the polarizability, so the greater the polarizability of the molecule, the higher is the dielectric constant [33]. Therefore, the polarizability increases with increase in HgS concentration.

Figure 5a, b shows the frequency dependence of dielectric constant (ϵ') for pure PVA and PVA/HgS nanocomposite at 0.04 M HgS content respectively, at different temperatures. From these figures, it is seen that the dielectric constant decreases with increasing frequency, but increases with increasing temperature. It is obvious that, at high frequency the (ϵ') values are nearly constant with frequency while, they still depend on temperature.

The increase of dielectric constant ϵ' with temperature can be attributed to the fact that the orientational polarization is connected with the thermal motion of molecules, so dipole molecules cannot orient themselves at lower temperature region. However, as the temperature increases, the orientation of dipoles is facilitated, which cause the increase of the degree of the dipole orientation and consequently enhance the value of the dielectric constant ϵ'

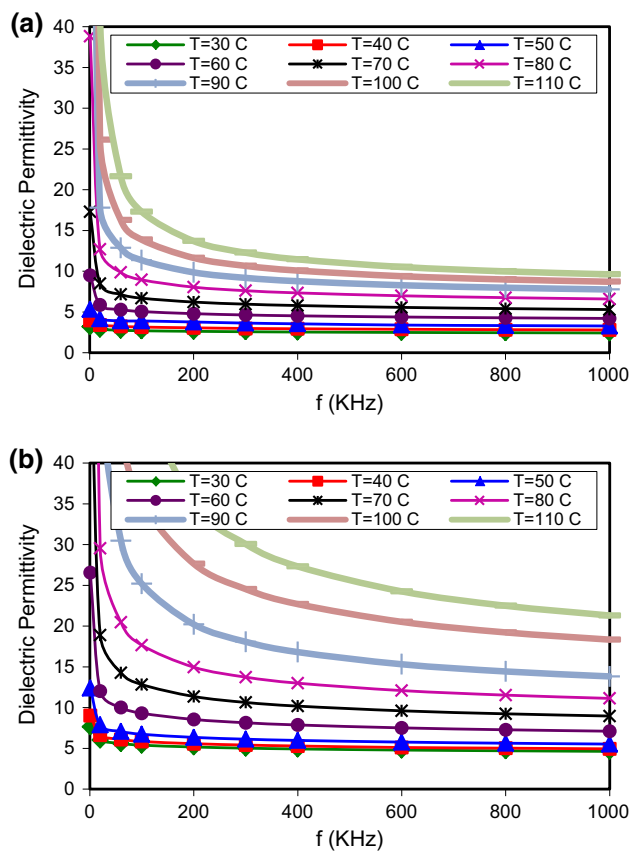


Fig. 5 Frequency dependence of dielectric constant (ϵ') at different temperatures for **a** pure PVA, and **b** PVA/HgS nanocomposite

[34]. In addition, the hydroxyl groups of PVA play a major role in ϵ'' [32].

3.5 Electrical conductivity

Electrical conduction of polymer nanocomposites has been calculated to gain insight into the nature of the charge transport in these materials. σ_{ac} is the ac-conductivity of the sample that arises from the motion of charge carriers through the polymer and is calculated according to [35, 36]:

$$\sigma_{ac} = dG_s/A$$

where, A is the effective cross-sectional area and G_s is measured conductance. The variation of ac-conductivity of PVA/HgS nanocomposites with the frequency of applied electric field at 30 °C is shown in Fig. 6. It can be observed that the addition of HgS increases and enhances the ac-conductivity (σ_{ac}) of PVA host, making the present study expected to be more useful in photonic and electronic device application. The ac-conductivity (σ_{ac}) is observed to be nearly independent at low frequencies followed by dispersion of the conductivity at higher frequency. The

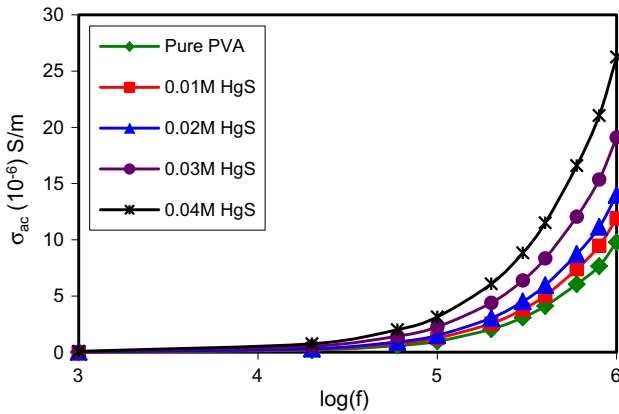


Fig. 6 Ac-Conductivity of PVA/HgS nanocomposites as a function of frequency, for different HgS concentrations at 30 °C

increase of ac-conductivity with frequency is a common phenomena for polymeric and semiconductor samples [36]. The frequency dependence of conductivity in polymer composites is due to hopping transport between the localized states [11].

To understand the conduction mechanism in PVA/HgS polymer nanocomposites, the frequency dependence of ac-conductivity σ_{ac} at various temperatures has been analyzed for the pure PVA and highest conducting sample (0.04 M HgS) and presented in Fig. 7.

It is clear from Fig. 7 that σ_{ac} increases with temperature. This suggested that the σ_{ac} is a thermally activated process from different localized states in the gap or its tail [37]. As the temperature increases polymer becomes soft and mobility of the main chain segments as well as the rotation of side groups become easier. Thus, at higher temperature more and more dipoles are oriented resulting in the higher equivalent surface charge density, as well as the charge migration increase, i.e. as the temperature increases the conductivity increases [38, 39]. In general, the obtained ac-conductivity results indicate that the ac-conductivity obeys the Jonscher's universal power law [40]:

$$\sigma = \sigma_{dc} + B\omega^s$$

where σ_{dc} is the frequency independent dc-conductivity, B is a dispersion temperature-dependent parameter, and s is a dimensionless frequency exponent, the typical values of (s) between 0 and 1, indicates the charge carrier interactions during hopping mechanism. The second term in this equation represents the ac-conductivity (σ_{ac}) [29].

The frequency exponent (s) value can characterize the type of electrical conduction mechanism, and the behavior of (s) value can be explained by many theoretical models. The exponent (s) values were calculated from the slop of $\log(\sigma_{ac})$ versus $\log(\omega)$ for all samples at different temperatures. The values of (s) versus temperature are presented in Fig. 8.

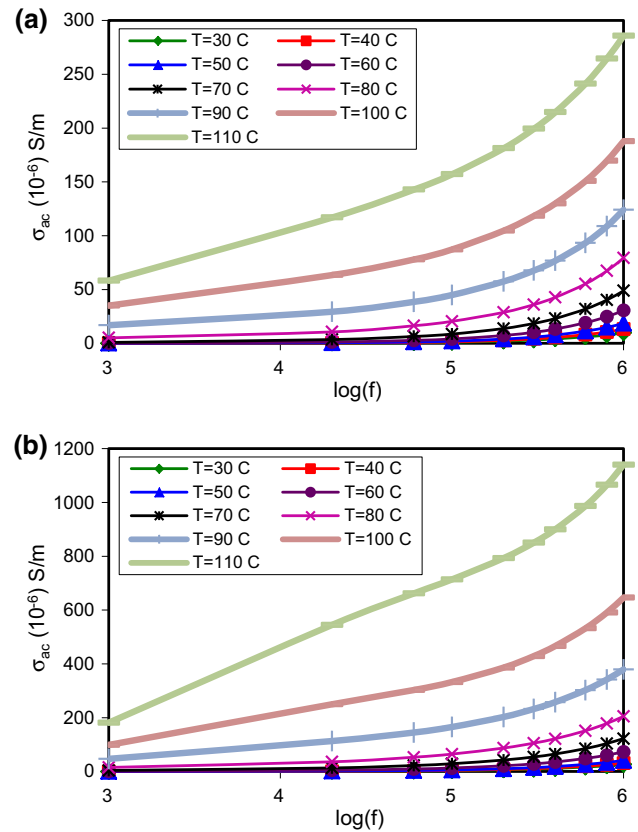


Fig. 7 Frequency dependence of ac-conductivity at different temperatures for **a** pure PVA and **b** PVA/HgS nanocomposite sample

It is clear from Fig. 8 that the value of s for all samples decreases with increasing temperature to a minimum value.

According to the quantum mechanical tunneling (QMT) model [41], the exponent (s) is almost equal to 0.8 and independent on temperature or slightly increases with increasing temperature. Therefore, QMT model is considered not applicable to the obtained results. According to the overlapping-large polaron tunneling (OLPT) model [42, 43], the exponent (s) is both frequency and temperature dependent, (s) decrease with increasing temperature from unity at room temperature to a minimum value at a certain temperature and then it increases with a further increase in temperature. Therefore, OLPT model is also not applicable to the obtained results.

According to correlated barrier hopping (CBH) model, values of the frequency exponent (s) is ranged from 1 to 0.7 at room temperature and have a tendency to decrease with increasing temperature [37]. This is in good agreement with the obtained results, so the frequency dependence of ac-conductivity (σ_{ac}) can be explained in terms of hopping of electrons between localized states at the Fermi level.

From Fig. 7, it is obvious that ac-conductivity σ_{ac} decreases with decreasing frequency, and become independent of

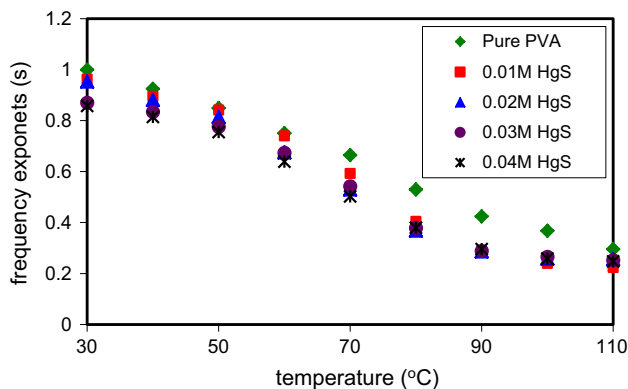


Fig. 8 The temperature dependence of the frequency exponents for PVA/HgS polymer nanocomposites films

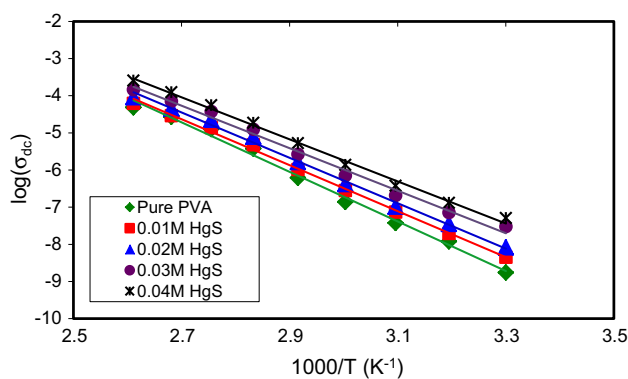


Fig. 9 Arrhenius plots of temperature dependence of σ_{dc} of PVA/HgS polymer nanocomposites

frequency after a certain value. Extrapolation of this part towards zero frequency will give σ_{dc} [44].

Figure 9 shows the variation of dc-conductivity σ_{dc} as a function of reciprocal temperature for pure PVA and PVA/HgS polymer nanocomposite films. It can be seen that the dc-conductivity increased with increasing temperature and HgS concentration, due to the increase in carriers mobility, and charge carriers density respectively, according to the Stokes–Einstein relation [45]. The σ_{dc} exhibit an Arrhenius behavior that can be described with the equation,

$$\sigma_{dc} = B' \exp(-E_{\sigma}/k_B T)$$

where E_{σ} denote the conductivity activation energies, k_B is Boltzmann constant (8.617×10^{-5} eV/K), T is the absolute temperature, and B' is proportionality constants which can be considered as the limiting value of conductivity at an infinite temperature [46]. The evaluated activation energy of the PVA/HgS polymer nanocomposite films, with correlation coefficient R^2 is recorded in Table 2. The R^2 values denoted that the data was fits accurately to the Arrhenius equation. The value of $E_{\sigma} = 0.575$ eV for pure PVA, which is in good agreement with that reported by other work [47].

Table 2 Activation energy E_{σ} , and correlation coefficient R^2 of the PVA/HgS solid polymer nanocomposites films

HgS (M)	E_{σ} (eV)	R^2 (regression value)
0	0.575	0.993
0.01	0.535	0.996
0.02	0.526	0.995
0.03	0.493	0.991
0.04	0.488	0.994

The activation energy of the conductivity is the minimum energy required to overcome the potential barrier in the composite system. It was clear that the activation energy values decreases slightly with increasing the HgS content. The activation energy decreases from 0.575 eV for pure PVA to 0.488 eV for 0.04 M HgS. Jonscher and Ansari [48] suggested that activation energy E_{σ} values less than 0.8 eV would indicate that the dominant charge transport is through the motion of electrons, whereas E_{σ} values higher than 0.8 eV reflect that the dominant charge transport is ionic [49]. Therefore, the present results indicate that the electron conduction mechanism is dominated in the present samples [50], which provide support to the previous proposed analysis. The decreases of activation energy which is due to the reduction of energy barrier to segmental motion of polymer matrix [51], confirm the transport in the present system is through a hopping mechanism [52], so the addition of HgS to PVA host enhances the electrical conduction due to electron contributions arising from the HgS.

4 Conclusions

PVA/HgS nanocomposites films with varying HgS content have been prepared successfully by in situ chemical reduction method and casting of aqueous solutions. FTIR studies confirmed the charge-transfer complex between PVA molecules and HgS nanoparticles. XRD analyzes revealed the formation of HgS crystal structure in the PVA film with an average diameter between 58.83 and 68.63 nm. The effects of the HgS concentration on the dielectric properties of the films were investigated. The high value of the dielectric constant and dielectric loss at low frequency was attributed to electrode polarization. The increases of electrical conductivity, dielectric constant, and dielectric loss with HgS concentration were deduced from data analysis, which corroborate towards the enhanced conducting behaviour of PVA matrix with an increase in the concentration of embedded HgS nanoparticles. The temperature dependence of ac-conductivity and variation of frequency exponent, suggests that the conduction

mechanism can be represented by the correlated barrier hopping (CBH) model. The Arrhenius behavior of dc-conductivity at investigated temperature region is due to hopping mechanism. The decrease of activation energy was observed with HgS concentrations.

Acknowledgments The Authors are very much grateful to the University of Sulaimani, for providing financial assistance for this research. The authors gratefully acknowledge the Kurdistan Institution for Strategic Studies and Scientific Research, and the Ministry of Science and Technology for the facility in their laboratories.

References

- P.W.M. Blom, H.F.M. Schoo, M. Matters, *Appl. Phys. Lett.* **73**, 3914–3916 (1998)
- X. Xu, E.R. Carraway, *Nanomater. Nanotechnol.* **2** Art. 17:2012 (2012)
- G.G. Roberts, E.L. Lind, E.A. Davis, *J. Phys. Chem. Solids* **30**, 833–844 (1969)
- H.C. Sinha, I.M. Talwar, A.P. Shrivastava, *Thin Solid Films* **82**, 229–234 (1981)
- M. Ravi, Y. Pavani, K.K. Kumar, S. Bhavani, A.K. Sharma, V.V.R.N. Rao, *Mater. Chem. Phys.* **130**, 442–448 (2011)
- A. Gautam, S. Ram, *Mater. Chem. Phys.* **119**, 266–271 (2010)
- C.C. Yang, G.M. Wu, *Mater. Chem. Phys.* **114**, 948–955 (2009)
- A.L. Saroj, R.K. Singh, *J. Phys. Chem. Solids* **73**, 162–168 (2012)
- O.Gh. Abdullah, D.A. Tahir, K. Kadir, *J. Mater. Sci. Mater. Electron.* **26**, 6939–6944 (2015). doi:10.1007/s10854-015-3312-9
- P.C. Mehendru, N.L. Pathak, K. Jain, P. Mehendru, *Phys. Status Solidi (a)* **42**, 403–407 (1977)
- H.N. Chandrakala, B. Ramaraj, Shivakumaraiah, G.M. Madhu, Siddaramaiah, *J. Alloys Compd.* **551**, 531–538 (2013)
- T. Kimura, M. Kajiwara, *J. Mater. Sci.* **33**, 2955–2959 (1998)
- A. Nigrawal, N. Chand, *Prog. Nanotechnol. Nanomater.* **2**, 25–33 (2013)
- X. Yuan, *Polym. Bull.* **67**, 1785–1797 (2011)
- A.S. Roy, S. Gupta, S. Sindhu, A. Parveen, P.C. Ramamurthy, *Compos. B* **47**, 314–319 (2013)
- C.A. Finch, *Polyvinyl alcohol properties and application* (Wiley, New York, 1973)
- S. Gunasekaran, E. Sailatha, S. Seshadri, S. Kumaresan, *Indian J. Pure Appl. Phys.* **47**, 12–18 (2009)
- S. Keskin, I. Uslu, T. Tunc, M. Ozturk, A. Aytimur, *Mater. Manuf. Process.* **26**, 1346–1351 (2011)
- Z. Ali, H. Youssef, T. Afify, *Polym. Compos.* **29**, 1119–1124 (2008)
- K.S. Hemalatha, K. Rukmani, N. Suriyamurthy, B.M. Nagabhushana, *Mater. Res. Bull.* **51**, 438–446 (2014)
- J. Xu, X. Cui, J. Zhang, H. Liang, H. Wang, J. Li, *Bull. Mater. Sci.* **31**, 189–192 (2008)
- R.P. Chahal, S. Mahendia, A.K. Tomar, S. Kumar, *J. Alloys Compd.* **538**, 212–219 (2012)
- H. Karami, M. Ghasemi, S. Matini, *Int. J. Electrochem. Sci.* **8**, 11661–11679 (2013)
- S. Sarma, P. Datta, *Nanosci. Nanotechnol. Lett.* **2**, 261–265 (2010)
- R. Selvaraj, K. Qi, S.M.Z. Al-Kindy, M. Sillanpaa, Y. Kim, C.W. Tai, *Royal Soc. Chem.* **4**, 15371–15376 (2014)
- S. Wu, C. Chen, X. Shen, G. Li, L. Gao, A. Chen, J. Hou, X. Liang, *Cryst. Eng. Comm.* **15**, 4162–4166 (2013)
- I. Saini, J. Rozra, N. Chandak, S. Aggarwal, P.K. Sharma, A. Sharma, *Mater. Chem. Phys.* **139**, 802–810 (2013)
- C. Brosseau, A. Beroual, A. Boudida, *J. Appl. Phys.* **88**, 7278 (2000)
- S.B. Aziz, Z.H.Z. Abidin, *Mater. Chem. Phys.* **144**, 280–286 (2014)
- V. Raja, A.K. Sharma, V.V.R.N. Rao, *Mater. Lett.* **58**, 3242–3247 (2004)
- T. Blythe, D. Bloor, *Electrical properties of polymers* (Cambridge University Press, Cambridge, 2005)
- K.P. Singh, P.N. Gupta, *Eur. Polym. J.* **34**, 1023–1029 (1998)
- M. Trihotri, U.K. Dwivedi, F.H. Khan, M.M. Malik, M.S. Qureshi, *J. Non-Cryst. Solids* **421**, 1–13 (2015)
- P.K. Khare, S.K. Jain, *Bull. Mater. Sci.* **23**, 17–21 (2000)
- J.C. Dyre, T.B. Schroder, *Rev. Mod. Phys.* **72**, 873–892 (2000)
- M.H. Harun, E. Saion, A. Kassim, M.Y. Hussain, I.S. Mustafa, M.A.A. Omer, *Malays. Polym. J.* **3**, 24–31 (2008)
- K. Ulutas, D. Deger, S. Yakut, *J. Phys. Conf. Ser.* **417**, 012040 (2013)
- OGH Abdullah, B.K. Aziz, A.O. Saeed, *Int. J. Sci. Adv. Technol.* **2**, 65–70 (2012)
- K. Dutta, S.K. De, *J. Nanopart. Res.* **9**, 631–638 (2007)
- J. Yang, X.J. Meng, M.R. Shen, L. Fang, J.L. Wang, T. Lin, J.L. Sun, J.H. Chu, *J. Appl. Phys.* **104**, 104113 (2008)
- A. Ghosh, *Phys. Rev. B* **41**, 1479 (1990)
- A.R. Long, *Adv. Phys.* **31**, 553–637 (1982)
- M.S. Aziz, A.G. Mostafa, A.M. Youssef, S.M.S. Youssif, *Phys. Res. Int.* **2011**, 1–10 (2011)
- D.K. Ray, A.K. Himanshu, T.P. Sinha, *Indian J. Pure App. Phys.* **43**, 787–793 (2005)
- S. Choudhary, R.J. Sengwa, *Indian J. Eng. Mater. Sci.* **19**, 245–252 (2012)
- OGH Abdullah, S.R. Saeed, *Chem. Mater. Res.* **3**, 19–24 (2013)
- N. Ahad, E. Saion, E. Gharibshahi, *J. Nanomater.* **2012**, Article ID 857569 (2012)
- A.K. Jonscher, A.A. Ansari, *Philos. Mag.* **23**, 205–223 (1971)
- A.K. Jonscher, *Thin Solid Films* **1**, 213–234 (1967)
- F.H.A. El-Kader, W.H. Osman, R.S. Hafez, *Phys. B* **408**, 140–150 (2013)
- M. Ravi, S. Bhavani, K.K. Kumar, V.V.R.N. Rao, *Solid State Sci.* **19**, 85–93 (2013)
- T.V. Kumar, A.S. Chary, S. Bhardwaj, A.M. Awasthi, S.N. Reddy, *Int. J. Mater. Sci. Appl.* **2**, 173–178 (2013)